Published in final edited form as:
*Science*. 2009 April 3; 324(5923): 59–63. doi:10.1126/science.1169494.

# Photodegradable hydrogels for dynamic tuning of physical and chemical properties

**April M. Kloxin**[1], **Andrea M. Kasko**[1,2,†], **Chelsea N. Salinas**[1], and **Kristi S. Anseth**[1,2]
April M. Kloxin: ; Andrea M. Kasko: ; Chelsea N. Salinas: ; Kristi S. Anseth: Kristi.Anseth@colorado.edu
[1]Department of Chemical and Biological Engineering, University of Colorado, 424 UCB ECCH 111, Boulder, CO 80309 USA, Phone: 303.492.7471, Fax: 303.735.0095
[2]Howard Hughes Medical Institute, University of Colorado, 424 UCB ECCH 111, Boulder, CO 80309 USA, Phone: 303.492.7471, Fax: 303.735.0095

## Abstract

We report a strategy to create photodegradable poly(ethylene glycol)-based (PEG) hydrogels through rapid polymerization of cytocompatible macromers for remote manipulation of gel properties in situ. Post-gelation control of the gel properties is demonstrated to introduce temporal changes, creation of arbitrarily shaped features, and on-demand pendant functionality release. Channels photodegraded within a hydrogel containing encapsulated cells allow cell migration. Temporal variation of the biochemical gel composition is utilized to influence chondrogenic differentiation of encapsulated stem cells. Photodegradable gels that allow real-time manipulation of material properties or chemistry provide dynamic environments with the scope to answer fundamental questions about material regulation of live cell function and may impact an array of applications from design of drug delivery vehicles to tissue engineering systems.

Hydrogels are hydrophilic polymers swollen by water that are insoluble owing to physical or chemical crosslinks. These water-swollen gels are used extensively as biomaterials for complex device fabrication (1), cell culture for tissue regeneration (2), and targeted drug release (3). Often, sophisticated control of the gel structure in space and time is required to elucidate the dynamic relationship between biomaterial properties and their influence on biological function (4,5). For example, progenitor cells are often expanded and differentiated in hydrogel microenvironments, and researchers have demonstrated how the initial gel properties, including mechanics (6,7) and chemical functionality (8), influence cellular fate. In regenerative medicine, the structure and composition of gels are also regulated temporally, through hydrolytic (9) and enzymatic (10-12) degradation mechanisms, to promote cell secretory properties and encourage the development of tissue-like structures in vitro and in vivo. A major challenge is determining which biochemical and biophysical features must be presented in a gel culture environment.

Hydrogel structure and functionality have evolved from the direct encapsulation of cells in simple homogeneous materials to those with highly regulated structures spanning multiple size scales (e.g., through self-assembly (13) or microengineering (14)). These hydrogel structures are further modified locally by cells with the synthetic incorporation of bioresponsive functionalities (15) or externally by advanced patterning to create spatially varying functionalities. For example, the chemical patterning of a gel by the addition of a second,

Correspondence to: Kristi S. Anseth, Kristi.Anseth@colorado.edu.
[†]Current address: Department of Bioengineering, University of California, Los Angeles, CA 90095-1600

interpenetrating network or peptide tether has been demonstrated by diffusing chemical moieties into a gel and covalently linking these functionalities to the network by photocoupling (16) or reaction with a photolytically uncaged reactive group (17). While these are important advances, such processes do not allow modulation of the gel chemistry in real-time or photodegradation of the gel structure. Few synthetic materials provide a cellular microenvironment in which physical or chemical cues are initially present and subsequently regulated on-demand. We have synthesized monomers capable of polymerizing in the presence of cells to produce photolytically degradable hydrogels whose physical or chemical properties are tunable temporally and spatially with light. The desired gel property for altering cell function or fabricating a device is thus externally-triggered and directed with irradiation by photolytic cleavage and removal of the macromolecules that comprise the gel.

The photodegradable functionality, a nitrobenzyl ether-derived moiety, was selected based on its photolytic efficiency, susceptibility to two-photon photolysis, and previous use in live cell culture and imaging (18,19). Similar photolabile functionalities have been used in multi-step gel modification processes (20). A base photodegradable monomer was synthesized by acrylation of the photolabile moiety via a pendant hydroxyl group (photodegradable acrylate, PDA, Fig. 1A) and was subsequently attached via a pendant carboxylic acid to PEG-*bis*-amine to create a photocleavable crosslinking diacrylate macromer (Compound 1, Fig. 1B) from which PEG-based photodegradable hydrogels (Fig. 1C) were synthesized. This approach, where the photolabile moiety is incorporated within the network backbone, is fundamentally different from strategies where reactive groups or biomolecules are asymmetrically caged or capped by a photolabile group (20). Here, the hydrogel itself is cleaved upon light exposure, decreasing the local network crosslink density and resulting in macroscopic property changes such as stiffness, water content, diffusivity, or complete erosion, all in the presence of cells.

The photodegradable crosslinker, Compound 1, was copolymerized with PEG monoacrylate (PEGA) in phosphate buffered saline (PBS) via redox-initiated free radical polymerization to create photodegradable hydrogels. Upon irradiation, these hydrogels release modified PEG, and after complete degradation they release modified poly(acrylate) chains, as shown in Fig. 1C. The bulk photodegradation of these hydrogels, ensured by flood irradiation through a small thickness of material, was characterized within a parallel-plate rheometer (21). The storage modulus ($G'$) is proportional to the hydrogel crosslinking density ($\rho_x$) (22,23), allowing calculation of the characteristic photolabile group degradation time ($\tau$) when normalized to its initial value ($G'_o$) via $G'/G'_o = \rho_x/\rho_{xo} = \exp(-2t/\tau)$. At an irradiation intensity of 10 mW/cm$^2$ at 365 nm, typical irradiation conditions for hydrogel photopolymerizations in the presence of cells (24), the hydrogel completely degrades in 10 minutes ($\tau \sim 280$ s, Fig. 1D). As expected from photolysis kinetics (supporting online text), doubling the intensity halves the time to complete degradation ($\tau \sim 140$ s, Fig. 1D), while irradiation at 405 nm increases the degradation time inversely with the relative molar absorptivity ($\tau \sim 930$ s, Fig. 1D). When the irradiation is ceased, the degradation is arrested; degradation is recommenced upon further irradiation (Fig. 1E). The degradation rate and extent and the resulting material properties such as stiffness thus can be predictably manipulated with light intensity and wavelength.

Precise control of gel crosslinking density was utilized to examine the influence of gel structure on cell spreading. Specifically, human mesenchymal stem cells (hMSCs) were encapsulated within a densely crosslinked gel where they exhibit a rounded morphology (Fig. 1F). When the gel crosslinking density was reduced through photodegradation, cell spreading was observed (Fig. 1G), while the cell viability was maintained (Fig. S4). Thus, cell morphology can be manipulated by irradiation and degradation of these hydrogels at any time in culture. While this control can be useful for allowing cell spreading or extracellular matrix (ECM) elaboration, this molecular scale degradation does not allow for bulk cell migration or long-range cell-cell interactions, which require fabrication of micron-scale channels by gel erosion.

To study gel erosion, degradation was first confined to the irradiation surface by selecting an irradiation wavelength that corresponds to a high photolabile group molar absorptivity (Fig. S1). Since the light intensity is highest within the uppermost layers of a thick gel, these top layers erode away rapidly during light exposure prior to degradation of underlying layers (see schematic, Fig. 2A). Irradiation of a hydrogel through a photomask degrades the material in the exposed regions and creates progressively recessed areas, whereas material in the unexposed areas remains intact (see photographic series, Fig. 2A). Profilometry reveals well-defined ridges, demonstrating reproduction of the irradiation pattern, and feature height increases linearly with exposure time (Fig. 2A). Such photolithographic techniques at highly absorbed wavelengths can be used to create surface features of varying height and width post-gelation, whilst avoiding concomitant dimension changes in the hydrogel bulk, useful for the fabrication and subsequent manipulation of cell culture devices.

Controlled creation of three-dimensional cell culture microenvironments facilitates the examination of cell-matrix and cell-cell interactions. The post-gelation addition of chemical moieties, such as peptides, to hydrogels in three dimensions has been demonstrated in a multi-step technique using a two-photon laser scanning microscope (LSM) (16,17). Using a photodegradable hydrogel in conjunction with a single (405nm) (Fig. S2) or two-photon (740nm) LSM (Fig. 2B), we generate three-dimensional features within a hydrogel by local photodegradation with scan parameters similar to those used for cell imaging and without the addition of chemical moieties. This rapid patterning (seconds to minutes) is achieved by controlled rastering of the laser focus within the hydrogel, locally degrading the polymer network and creating arbitrary three-dimensional features on the micron scale (schematic, Fig. 2B). Interconnected channels, potentially useful for directing cell connectivity and/or migration, were created within a rhodamine-labeled photodegradable hydrogel with a two-photon LSM and visualized using brightfield and fluorescence microscopy (Fig. 2B). Other features of arbitrary shape and size for desired applications such as device fabrication can be precisely and rapidly patterned within these photodegradable hydrogels in situ using either a single or two-photon LSM with standard imaging parameters (Fig. S2).

To demonstrate how erosion of these photodegradable hydrogels can be used to direct cell migration, fibrosarcoma cells were encapsulated within a hydrogel. A portion of these entrapped cells was subsequently released by degrading channels within the gel using photolithography. Cells near the periphery of the channel or released by erosion of the channel were then allowed to migrate along the channel length (Fig. 2C). With the ability to pattern micro to macroscopic structures in the presence of encapsulated cells, these photodegradable hydrogels provide a cell culture platform to allow unique studies of directed cell migration (25,26) and cell connectivity (27) by enabling real-time manipulation of the cell microenvironment. It is important to note, however, that cell migration exclusively occurs in regions of complete or near-complete gel erosion. In many cases, the culturing of cells in an environment that allows bulk migration is desirable with subsequent direction of cell-cell interactions at a certain point in time or space. To achieve this, complementary chemistries, such as enzymatically degradable moieties, can be incorporated within these gels by, for example, Michael addition (9) of the photodegradable crosslinker with an enzymatically cleavable, thiol-containing peptide (2).

The aforementioned techniques have focused on the patterning of hydrogels for degradation of the physical network structure; however, photodegradable linkages can also be exploited to locally modify the chemical environment within a hydrogel via incorporation of tethered, but photolabile, biologically active functionalities. To demonstrate, the PDA monomer was coupled through its pendant carboxylic acid to the ubiquitous adhesion peptide sequence RGDS (28), producing an asymmetric, photodegradable, biofunctional acrylic monomer (Fig. 3A). Copolymerization of this photo-releasable macromer with a non-degradable PEG diacrylate

(PEGDA) yields a hydrogel with photolytic control over its chemical interaction with encapsulated cells (Fig. 3B). Upon irradiation, the modified peptide is cleaved from the polymer network and released into solution, where it quickly diffuses out of the gel (Fig. S3). Peptide presentation within the microenvironment can thus be controlled with irradiation at a rate based on the photolabile group characteristic degradation time (Fig. 1D). More generally, this technique can be used for controlling the chemical structure of hydrogels in three dimensions and in time, where the peptide RGDS can be replaced with any biomolecule of interest, creating an additional tool for the modulation of ligand presentation (4).

To demonstrate the utility of this photolabile tether platform, hMSCs were encapsulated in non-degradable PEGDA hydrogels, both with and without the photoreleasable RGDS moiety, to examine the effect of temporal RGDS presentation on hMSC viability and chondrogenic differentiation. Control of the local biochemical environment enables promotion of chondrogenesis. While numerous researchers have incorporated the fibronectin epitope RGD into biomaterial microenvironments to promote the survival of hMSCs (5,29,30), few studies investigate the importance of the persistence of this signal on the differentiation fate (31-33). Natively, hMSCs differentiating into chondrocytes initially produce the adhesion protein fibronectin, which is subsequently downregulated between Day 7 and 10 while the excreted ECM is remodeled through enzyme production (31,34). After Day 10, these cells upregulate production of glycosaminoglycans (GAGs) and type II collagen (COLII), two major components of cartilage and specific indicators of chondrogenic differentiation (31,34). To examine this temporal change in vitro, a portion of the cell-gel constructs containing the photolabile RGDS tether were irradiated on Day 10 in culture to remove the fibronectin epitope RGDS from the encapsulated cell microenvironment (Fig. 3B).

The absence of RGDS in three dimensional cell culture yields a statistically significant decrease ($p<0.05$) in hMSC viability within the first 7 days in PEG-only gels (see inset, Fig. 3C), in agreement with other experimental results (29,30) (supporting online text). Upon photolytic removal of RGDS from the photolabile tether gels on Day 10, cell viability was unaffected; however, by day 21, a four-fold statistical increase ($p<0.05$) in the production GAGs occurred relative to the persistently presented RGDS or PEG-only hydrogels, indicating further differentiation of the hMSCs down the chondrogenic pathway in response to the microenvironment modification (Fig. 3C,Fig. S5). To examine cell interaction with this dynamic microenvironment, fixed sections were immunostained for the expression of the $\alpha_v\beta_3$ integrin, one of the cell surface integrins by which cells interact with RGDS. Cells persistently presented with RGDS express the integrin while most cells with RGDS photoreleased cease integrin expression by Day 21 (Fig. 4A), indicating that the cells have locally sensed and responded to the chemical change in their environment. Additionally, to determine that the elevated GAG production is associated with chondrogenesis, sections of the cell-hydrogel constructs were immunostained for the hMSC marker CD105 (TGFβ receptor) and the chondrocyte marker COLII. As hMSCs differentiate into chondrocytes in three-dimensional culture, a decrease in CD105 expression is observed along with onset of COLII production (35). The photolytic removal of RGDS on Day 10 is accompanied by a decrease in CD105 expression and elevated COLII production as compared to persistently presented RGDS on Day 21 (Fig. 4B), indicating increased chondrogenesis. With this photodegradable tether approach, the dynamic influence of other biomolecules on cell function can be similarly studied, expanding the ability to fabricate material environments that control cell function. While manipulation of a single signal was examined and utilized to direct hMSC differentiation herein, this gel system can be readily functionalized with photolabile moieties of different light absorbances and cleavage efficiencies, enabling independent control over multiple signals via selection of irradiation wavelength and intensity.

We have demonstrated the synthesis of photodegradable macromers and their subsequent polymerization to form hydrogels whose physical, chemical, and biological properties can be tuned in situ and in the presence of cells via UV, visible, or two-photon irradiation. These photodegradable hydrogels show promise as in vitro three-dimensional cell culture platforms where cell-material interactions are dynamically and externally directed to elucidate how cells receive and process information from their environment. Ways to promote or suppress desired cell functions may become possible with temporal and spatial regulation of the 3D culture microenvironment, leading to applications in fields ranging from controlled drug delivery to tissue regeneration.

## Supplementary Material

Refer to Web version on PubMed Central for supplementary material.

## Acknowledgments

The authors would like to thank C. Bowman, T. Scott, and C. Kloxin for comments on early versions of this manuscript and valuable discussions; A. Aimetti for peptide synthesis training; J. McCall and S. Anderson for cell culture assistance; M. Schwartz for cell migration discussions; C. Bowman and his laboratory for use of and assistance with the rheometer and profilometer; C. Kloxin for assistance with image analysis; C. DeForest, Carl Zeiss, Inc., and the Howard Hughes Medical Institute Janelia Farms campus for assistance with and use of the Zeiss 710 two-photon confocal LSM; and the Howard Hughes Medical Institute and the NIH (grants DE12998 and DE16523) for research support. A. Kloxin thanks the NASA GSRP fellowship and the DoEd GAANN fellowship for support. A patent related to this work has been submitted (U.S. Patent Application No. 11/374,471).

## References and notes

1. Weibel DB, DiLuzio WR, Whitesides GM. Nat Rev Microbiol Mar;2007 5:209. [PubMed: 17304250]
2. Lutolf MP, Hubbell JA. Nat Biotechnol Jan;2005 23:47. [PubMed: 15637621]
3. Langer R, Peppas NA. Aiche J Dec;2003 49:2990.
4. Stevens MM, George JH. Science Nov 18;2005 310:1135. [PubMed: 16293749]
5. Chan G, Mooney DJ. Trends Biotechnol Jul;2008 26:382. [PubMed: 18501452]
6. Engler AJ, Sen S, Sweeney HL, Discher DE. Cell Aug 25;2006 126:677. [PubMed: 16923388]
7. Engler AJ, et al. J Cell Biol Sep 13;2004 166:877. [PubMed: 15364962]
8. Kenny PA, Bissell MJ. Int J Cancer Dec 10;2003 107:688. [PubMed: 14566816]
9. Metters A, Hubbell J. Biomacromolecules Jan-Feb;2005 6:290. [PubMed: 15638532]
10. Rice MA, Sanchez-Adams J, Anseth KS. Biomacromolecules Jun;2006 7:1968. [PubMed: 16768421]
11. Seliktar D, Zisch AH, Lutolf MP, Wrana JL, Hubbell JA. J Biomed Mater Res Part A Mar 15;2004 68A:704.
12. Ehrbar M, et al. Circ Res Apr 30;2004 94:1124. [PubMed: 15044320]
13. Silva GA, et al. Science Feb 27;2004 303:1352. [PubMed: 14739465]
14. Khademhosseini A, Langer R. Biomaterials Dec;2007 28:5087. [PubMed: 17707502]
15. Sands RW, Mooney DJ. Curr Opin Biotechnol Oct;2007 18:448. [PubMed: 18024105]
16. Hahn MS, Miller JS, West JL. Adv Mater Oct 17;2006 18:2679.
17. Wosnick JH, Shoichet MS. Chem Mat Jan 8;2008 20:55.
18. Zhao YR, et al. Journal of The American Chemical Society Apr 14;2004 126:4653. [PubMed: 15070382]
19. Alvarez M, et al. Adv Mater Dec;2008 20:4563.
20. Luo Y, Shoichet MS. Nat Mater Apr;2004 3:249. [PubMed: 15034559]
21. Khan SA, Plitz IM, Frantz RA. Rheol Acta Mar-Apr;1992 31:151.
22. Young, RJ.; Lovell, PA. Introduction to polymers. Vol. 2nd. Chapman & Hall; London, U. K.: 1991. p. 443

23. Bryant, SJ.; Anseth, KS. Scaffolding in Tissue Engineering. Ma, PX.; Elisseeff, J., editors. Marcel Dekker, Inc.; 2005.
24. Bryant SJ, Nuttelman CR, Anseth KS. J Biomater Sci-Polym Ed 2000;11:439. [PubMed: 10896041]
25. Tayalia P, Mendonca CR, Baldacchini T, Mooney DJ, Mazur E. Adv Mater Dec;2008 20:4494.
26. Raeber GP, Lutolf MP, Hubbell JA. Biophys J Aug;2005 89:1374. [PubMed: 15923238]
27. Mahoney MJ, Anseth KS. Biomaterials Apr;2006 27:2265. [PubMed: 16318872]
28. Ruoslahti E, Pierschbacher MD. Science Oct 23;1987 238:491. [PubMed: 2821619]
29. Boontheekul T, Mooney DJ. Curr Opin Biotechnol Oct;2003 14:559. [PubMed: 14580589]
30. Hudalla GA, Eng TS, Murphy WL. Biomacromolecules Mar;2008 9:842. [PubMed: 18288800]
31. Tavella S, et al. J Cell Sci Sep;1997 110:2261. [PubMed: 9378775]
32. Nuttelman CR, Tripodi MC, Anseth KS. Matrix Biol May;2005 24:208. [PubMed: 15896949]
33. Salinas CN, Anseth KS. Biomaterials 2008;29:2370. [PubMed: 18295878]
34. DeLise AM, Fischer L, Tuan RS. Osteoarthritis Cartilage Sep;2000 8:309. [PubMed: 10966838]
35. Salinas CN, Cole BB, Kasko AM, Anseth KS. Tissue Eng May;2007 13:1025. [PubMed: 17417949]

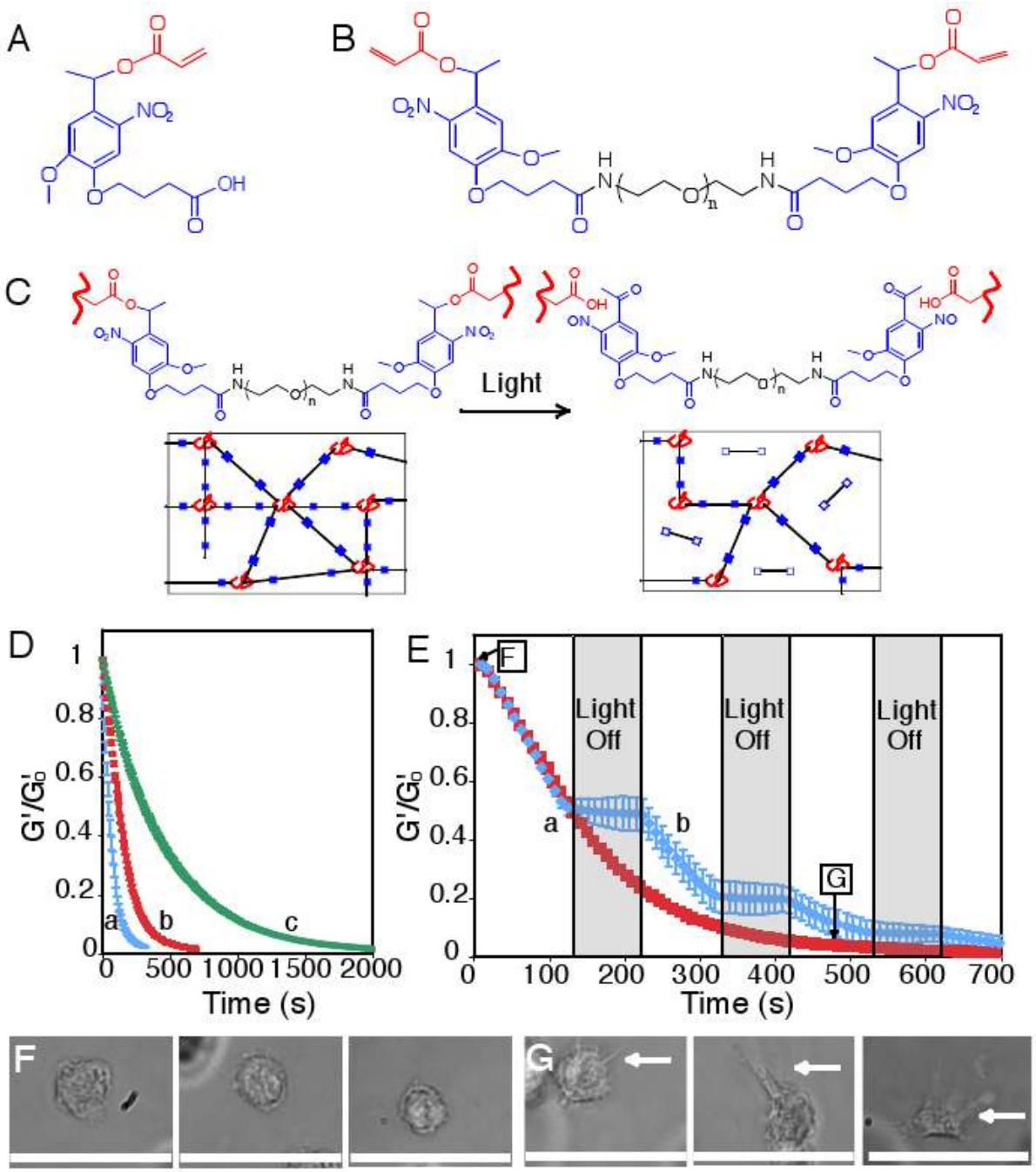


**Figure 1. Photodegradable hydrogel synthesis and degradation for tuning gel properties**

**(A)** The base photodegradable acrylic monomer was used to synthesize **(B)** the photodegradable crosslinking macromer (Compound 1, $M_n$ ~ 4070 g/mol), comprised of PEG (black), photolabile moieties (blue), and acrylic end groups (red). **(C)** Compound 1 was copolymerized with PEGA ($M_n$ ~ 375 g/mol), creating gels composed of poly(acrylate) chains (red coils) connected by PEG (black lines) with photolabile groups (solid blue boxes) (left). Upon irradiation, the photolabile moiety cleaves (open blue boxes), decreasing $\rho_x$ and releasing modified PEG (right). **(D)** The physical structure of the hydrogel is degraded via photolysis, decreasing $\rho_x$ and G′. The influence of irradiation on G′, normalized to $G'_o$, was monitored

with rheometry. The degradation rate was precisely controlled with irradiation intensity and wavelength: (a) 365 nm at 20 mW/cm$^2$, (b) 365 nm at 10 mW/cm$^2$, and (c) 405 nm at 25 mW/cm$^2$. **(E)** The gel degradation was modulated by either (a) continuous or (b) periodic irradiation with 365 nm at 10 mW/cm$^2$. The extents of degradation corresponding to the materials used in Fig. 1F and 1G are indicated. **(F)** hMSCs encapsulated within dense hydrogels exhibit a rounded morphology. **(G)** Irradiation (480 s, 365 nm at 10 mW/cm$^2$) significantly degrades the gel ($\rho_x/\rho_{xo} \sim 0.04$), promoting hMSC spreading after 3 days in culture. Scale bar, 50 μm.

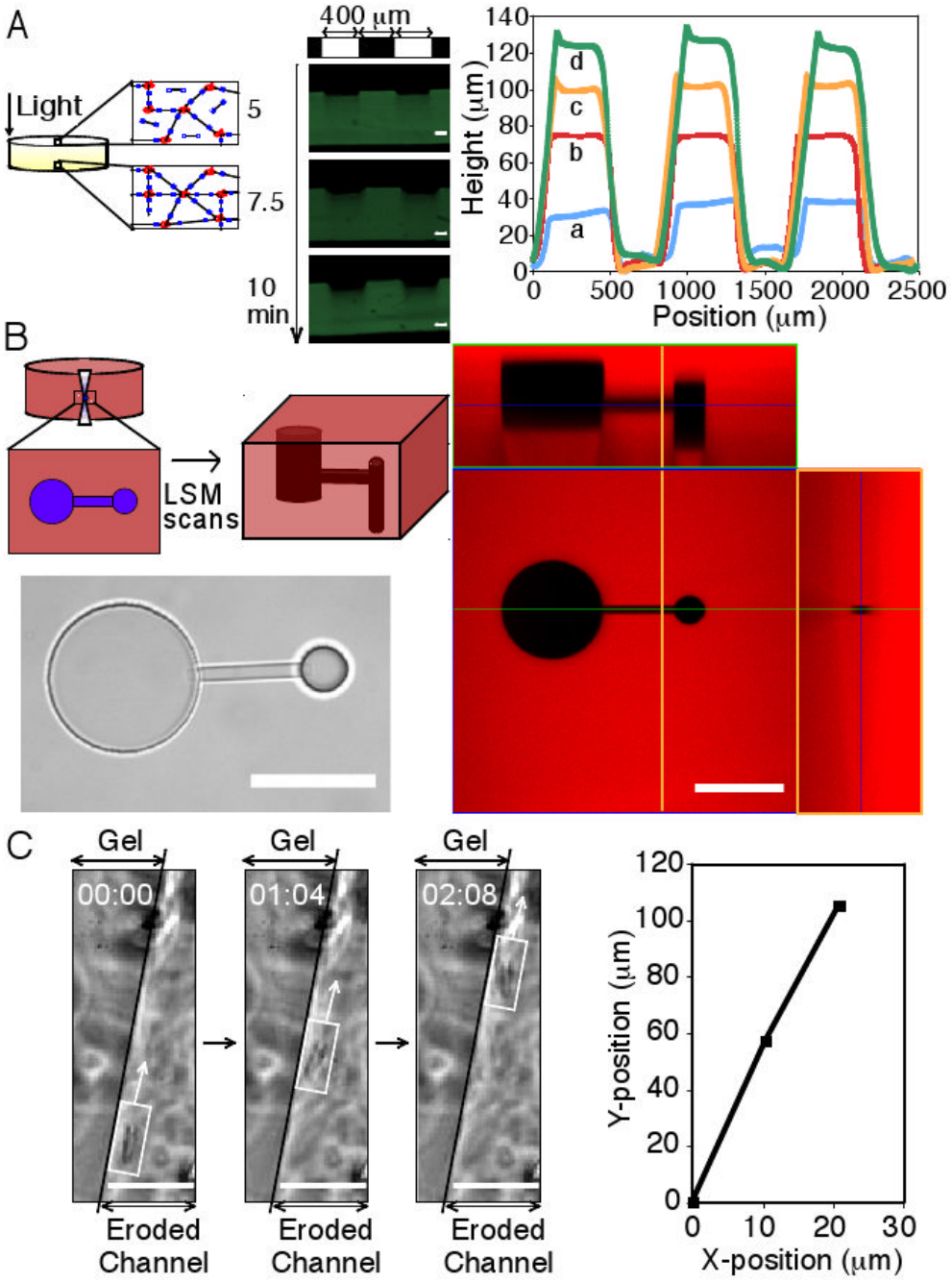


**Figure 2. Two and three-dimensional patterning of photodegradable hydrogels**

**(A)** Thick gels demonstrate surface erosion upon irradiation (left). A gel covalently labeled with fluorescein was eroded spatially via masked flood irradiation (320-500 nm at 40 mW/cm$^2$, 400 μm line periodic photomask). Channel depth increased linearly with irradiation, and no changes in hydrogel dimensions due to increased swelling were observed (middle). Feature dimensions were quantified with profilometry: (a) 2.5, (b) 5, (c) 7.5, and (d) 10 minutes irradiation (right). Scale bar, 100 μm. **(B)** Interconnected three-dimensional channels were fabricated within a photodegradable gel, covalently labeled with rhodamine B, using a two-photon LSM. A thin horizontal channel connected two offset vertical channels of different diameter, which was visualized in brightfield (bottom left) and with confocal LSM (right, intact

gel is red and the created feature is black, corresponding cross-sections are noted by blue, green, and orange lines). Scale bar, 100 μm. **(C)** Channels were eroded within a hydrogel encapsulating fibrosarcoma cells, releasing cells into the degraded channel and enabling migration. Migration of a cell along the edge of a channel is shown in time-lapsed brightfield images (left) and its corresponding position trace (right). Scale bar, 50 μm.

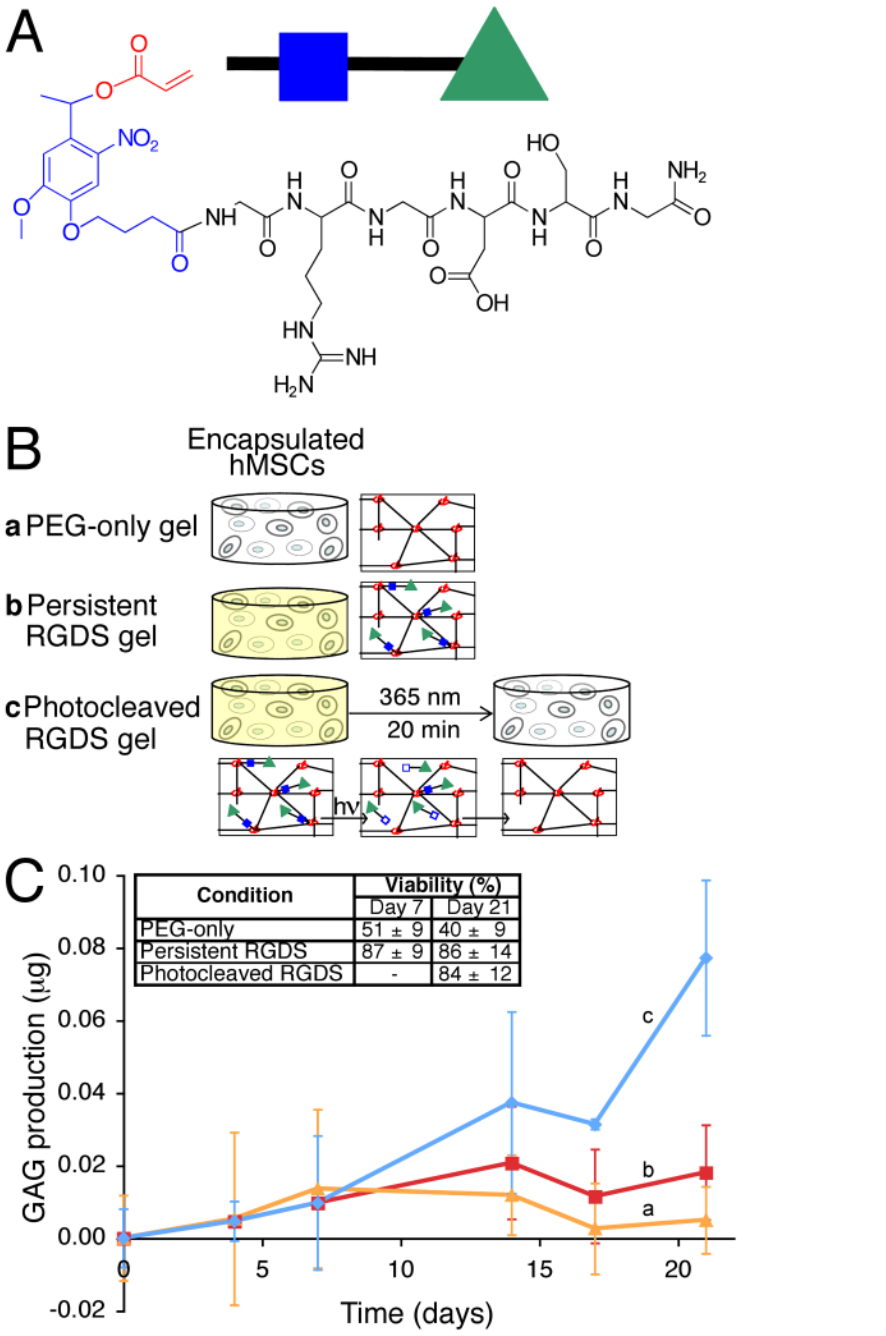


**Figure 3. Photolabile RGDS tether synthesis and utilization for dynamic changes in microenvironment chemistry**

**(A)** A photolabile asymmetric biofunctional acrylic monomer (Compound 2) was synthesized containing the adhesion peptide RGDS (black) attached to the PDA (acrylate in red and photolabile moiety in blue). **(B)** Compound 2 was polymerized (green triangle with closed blue box) into a non-degradable gel (red poly(acrylate) coils connected by black non-degradable PEG crosslinks) whose chemical composition is controlled with light exposure by photolytic release of the tethered biomolecule RGDS (bottom, green triangle with open blue box). hMSCs were encapsulated in non-degradable PEG gels (b) with or (a) without photoreleasable RGDS. The presentation of RGDS was temporally altered by (c) photocleavage of RGDS from the gel

on Day 10 in culture. **(C)** RGDS presentation maintains hMSC viability within PEG-based gels (inset table). RGDS photolytic removal on Day 10 directs hMSC chondrogenesis, (c) increasing GAG production four-fold over (b) persistently-presented RGDS or (a) PEG-only gels by Day 21 ($p<0.05$), an indicator of hMSC chondrogenesis.

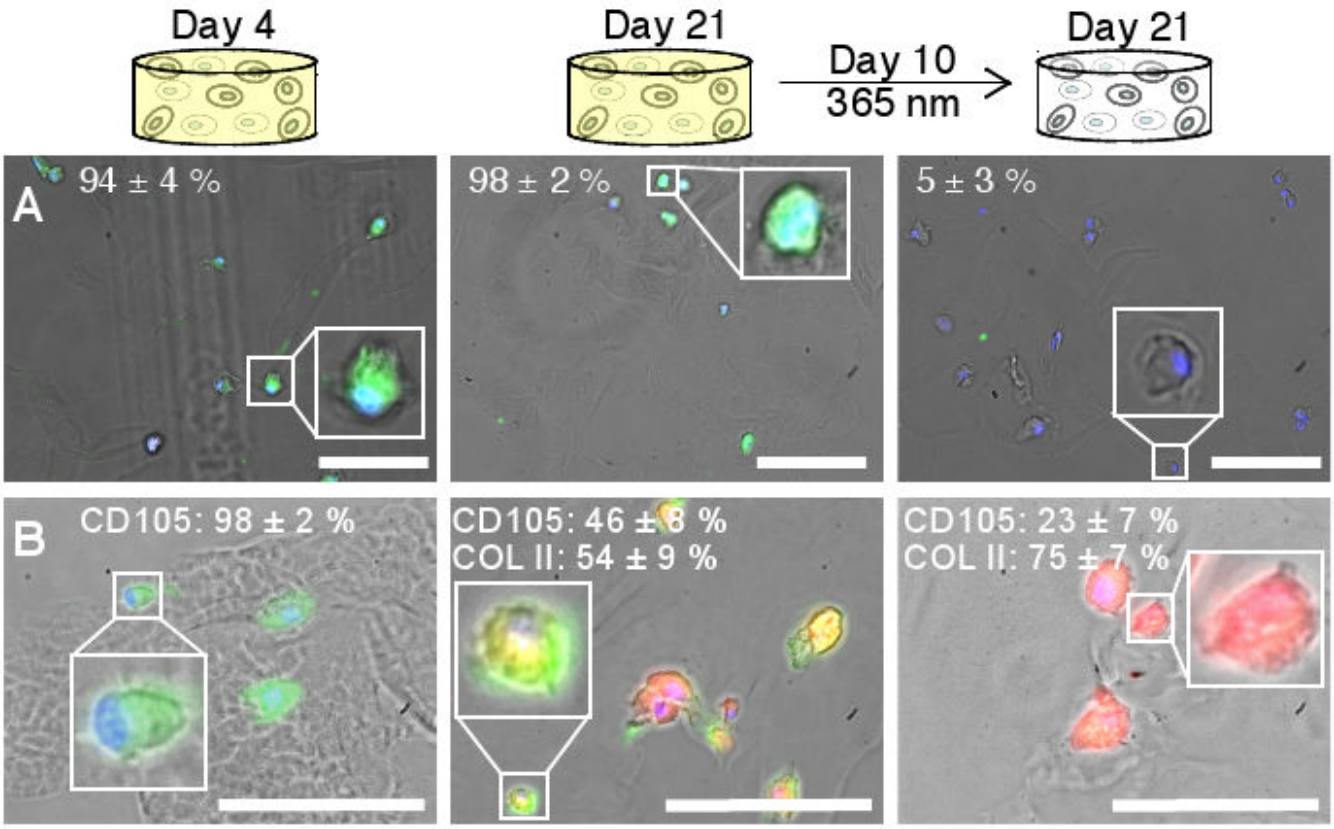


**Figure 4. Influence of dynamic microenvironment chemistry on integrin expression and differentiation**

**(A)** Cells (DAPI-labeled nuclei, blue) cultured with persistent RGDS express the cell-surface integrin $\alpha_v\beta_3$ (FITC-labeled, green) on at Day 4 (left) and Day 21 (middle) in culture. Cells with photocleaved RGDS have decreased expression of the $\alpha_v\beta_3$ integrin by Day 21 (right), indicating that the cells have responded to the removal of RGDS. (Representative images shown with average cell percentages noted.) **(B)** Chondrogenic differentiation of hMSCs was verified by immunostaining for the hMSC marker CD105 (FITC, green) and the chondrocyte marker COLII (TRITC, red). Within error, no cells initially produce COLII (Day 4, left). By Day 21, half of the cells presented persistently with RGDS strongly expressed CD105 and the other half produced COLII (middle). With photolytic removal of RGDS on Day 10, one-fourth of the cells strongly expressed CD105 and three-fourths produced COLII (right), supporting that photolytic removal of RGDS increases chondrogenesis. (Representative images shown with average cell percentages strongly expressing the marker noted.) Scale bars, 100 μm.